

Gravity wave climatology and trends at 85-110 km deduced from Collm low-frequency ionospheric E-region drift measurements 1984-2003

Christoph Jacobi, Dierk Kürschner, Nikolai M. Gavrilov

Zusammenfassung

Die Schwerewellenaktivität in der oberen Mesosphäre und unteren Thermosphäre wird mit Hilfe von ionosphärischen Driftmessungen im Zeitraum 1984-2003 unter Verwendung eines kommerziellen Rundfunksenders untersucht. Der Reflexionspunkt in der unteren Ionosphäre ist bei 52.1°N, 13.2°E, die Messhöhe ist 85-110 km. Die Ergebnisse zeigen maximale Aktivität in der sommerlichen Mesosphäre, wobei sich das Maximum in größeren Höhen zu den Äquinoktien hin verschiebt. Dieser Bereich maximaler Schwerewellenamplituden deckt sich mit demjenigen der größten vertikalen Scherung des Hintergrundwindes. Die Ausbreitungsrichtung ist vorzugsweise west-östlich, mit einer südöstlichen Komponente im Winter in der Mesosphäre und einer nordöstlichen Komponente im Sommer in der unteren Thermosphäre. Die Zeitreihen der 3-monatig gemittelten Schwerewellenaktivität zeigen maximale Amplituden um 1989-2001 und 2000-2002, was auf einen möglichen Einfluss des 11-jährigen Sonnenfleckenzyklus auf die dynamische Aktivität der Mesosphäre und unteren Thermosphäre hinweist.

Summary

Gravity wave activity obtained from lower ionospheric drift measurements in the height range 85-110 km at 52.1°N, 13.2°E during 1984-2003 are presented. The results show maximum activity in the mesosphere in summer, with a shift to equinoxes at higher altitudes. Maximum gravity wave amplitudes are found near the regions of strongest vertical mean wind shear. The propagation direction is generally close to E-W, however, during winter at lower heights a more South-Easterly direction is preferred, while at greater heights during summer a North-Easterly direction is visible. Time series of seasonal (3-monthly) mean zonal drift variances show maximum amplitudes around 1989-1991 and 2000-2002, which is concomitant with the solar activity maxima within the 11-year solar cycle.

Introduction

Internal gravity waves (GW) are the important process that controls the dynamics and temperature field of the mesosphere and lower thermosphere (MLT). GW are filtered by the mean circulation in the stratosphere and mesosphere, and accelerate the mean flow in the mesosphere, which leads to the lower thermospheric zonal wind reversal, meridional circulation and low summer MLT temperatures that cannot be explained without taking into account the effect of breaking gravity waves. Successful modelling of MLT dynamics therefore requires knowledge of GW fluxes and their seasonal and vertical distribution. While some first global climatologies of stratospheric GW activity are available from satellite measurements (Tsuda et al., 2000; McLandress et al., 2000; Venkat Ratnam et al., 2004), analyses of GW activity in the MLT essentially relies on ground-based measurements so that basically local climatologies are available. Fewer studies involve regional or global variability (Manson et al., 2002, 2004). The relative sparseness of multi-instrument studies is, among others, due to peculiarities of the different measuring systems (radars of different wavelength, optical) that allow the detection of GW in different spectral ranges or in different parameters.

Nevertheless, comparatively many publications have dealt with the seasonal variations of GW as obtained from radar measurements (Gavrilov et al., 1995, 2001, 2002; Manson et al., 1997, 1999, 2003; Gavrilov and Jacobi, 2004), and also with the comparison of GW activity in the course of the year over different stations. These works may provide an average climatology of GW although the spectral ranges considered depend on the measuring principle used. For example, medium frequency (MF) radars are able to measure winds with a time resolution of few minutes, while the low-frequency (LF) method only provides wind variances in a period window between 0.7 and 3 hours (Gavrilov et al., 2001). Therefore, if a global picture is constructed from the individual radar measurements, the result may be somewhat qualitative. At midlatitudes, in the mesosphere a semiannual oscillation (SAO) of GW activity with maxima in winter and summer is usually found, with the summer maximum being more pronounced for longer GW periods (Gavrilov et al., 2002). The SAO may be explained by the middle atmosphere jets that lead to large intrinsic phase speeds and therefore larger wind variances (Manson et al., 1997). One of the most powerful methods of detecting GW in the mesosphere is using MF radar measurements, owing to their high temporal resolution and long-term reliability with few data gaps. However, MF radars usually measure up to altitudes around 95 km, so that above that level measurements are sparse. Analyses of low-frequency (LF) drifts have shown that near 100 km the SAO phase shifts with GW amplitude maxima near solstices (Gavrilov et al., 2001).

GW measured at MLT heights are on the one hand dependent on their sources, which are mainly situated in the troposphere (Nastrom and Fritts, 1992a,b), although e.g. Gavrilov and Jacobi (2004) have shown that middle atmosphere GW sources may play an important role in establishing the observed seasonal distribution. On the other hand in particular GW with small phase speeds are sensitive to wind filtering in the middle atmosphere (Taylor et al., 1993). This is especially true for middle and high latitudes, where the stratospheric and mesospheric zonal winds are strong, while the low-latitude MLT GW activity seems to be more strongly controlled by the GW sources in the lower atmosphere (Manson et al., 1999). Nevertheless, even for midlatitudes especially considering long-period GW their MLT activity and (spatial and temporal) variability is resulting from a mixture of source distribution and middle atmosphere filtering.

One method of revealing the relative influence of GW sources and mean wind filtering on the MLT wind variance distribution is analysing long-term variability of GW and comparison with atmospheric mean circulation or characteristic circulation patterns at different heights. Long-term analyses of GW activity in the MLT, however, are sparse. Gavrilov et al. (1995) analysed 15 years of midlatitude MF radar data. Gavrilov et al. (1999) analysed 12 years of data measured over Japan, while low-latitude measurements over Hawaii (11 years) have been presented by Gavrilov et al. (2004). Major focus of these studies is the presentation of the seasonal and vertical variation of GW over the respective stations. Only few studies explicitly included the analysis of interannual variability on time scales of few years, in particular since the time series available are short, so that conclusions are preliminary. A possible 11-year solar cycle effect was mentioned by Gavrilov et al. (1995), however, comparison of 3 midlatitude stations by Gavrilov et al. (2002) showed that there are substantial differences between longitudes. A relatively strong effect of the Southern Oscillation (SO) was shown by Gavrilov et al. (2004) for Hawaii MF radar data, while the interannual variation of GW over Japan also indicated a possible, although less pronounced, influence of the SO (Gavrilov and Fukao, 2001).

Notwithstanding the great number of publications showing GW climatologies and comparisons between stations, one of the major results is the strong variability of GW activity and

parameters as propagation direction also across relatively short distances, which is assumed to be connected either with different wind filtering or local sources (Manson et al., 2003, 2004). Therefore, further long-term measurements are required. Here we present GW analyses using a 20-year database measured at Collm, Germany, using the LF method. The dataset represents an update of that one presented by Gavrilov et al. (2001) that was also used in the comparison study by Gavrilov et al. (2002) and have been compared to model results by Gavrilov and Jacobi (2004). Including roughly another half of a solar cycle enables us to draw more substantial conclusions on interannual variability of GW over Central Europe.

Database

The wind field of the upper mesopause region is continually observed by daily radio drift and reflection height measurements in the LF range, using the ionospherically reflected sky wave of commercial radio transmitters on 177, 225 and 270 kHz. The measurements are carried out according to the closely-spaced receiver technique. A modified form of the similar-fade method is used to interpret the wind measurements (Kürschner, 1975; Schminder and Kürschner, 1994). The procedure is based on the estimation of time differences between corresponding fading extrema for three measuring points forming a right angled triangle over the ground with small sides of 300 m in direction N and E, respectively. The individual pairs of time differences which allow the calculation of individual wind vectors are measured at a temporal resolution of 0.25 s.

The data are combined to half-hourly zonal (u) and meridional (v) mean drift values on each frequency, with a mean value being averaged over 30-60 data points. The $1-\sigma$ variation of the half-hourly mean, with σ being the standard deviation, is in the order of 20 ms^{-1} , caused by the real wind variations, the resolution and number of the individual wind measurements, and some statistic uncertainties connected with properties of ionospheric irregularities and additionally turbulent motions.

The virtual reflection height h' is measured on 177 kHz (transmitter Zehlendorf, reflection point at 52.1°N , 13.2°E) using travel time differences between the ground wave and the sky wave. The differences are obtained using side-band phase comparisons of both wave components in the modulation frequency range near 1.8 kHz (Kürschner et al., 1987). The uncertainty of an individual reflection height measurement is nearly 2 km. The half-hourly means consist of 6000 individual values on an average. Essentially caused by the variability of reflection heights the $1-\sigma$ variation of the half-hourly mean is in the order of 3 km below 95 km and 5 km near 100 km height.

Gravity wave analysis

The LF method delivers measurements of zonal, u , and meridional, v , drift velocities at one height at a time, with data gaps during daylight hours essentially caused by D region absorption especially in the summer months. The height is changing systematically during the day (e.g. Kürschner, 1987), so that the construction of a time series and deviations from the daily mean value is not possible. Therefore the basis of the gravity wave analysis are the differences of the two consecutively measured half-hourly mean drift velocities on 177 kHz:

$$u'(t) = u\left(t + \frac{\Delta t}{2}\right) - u\left(t - \frac{\Delta t}{2}\right), \quad (1)$$

$$v'(t) = v\left(t + \frac{\Delta t}{2}\right) - v\left(t - \frac{\Delta t}{2}\right), \quad (2)$$

with $\Delta t = 30$ min. These values are only used if the height difference Δh between the two drift velocities used is 2 km or less. The u'^2 and v'^2 data are then averaged over a height range of 10 km and the respective time interval under consideration. The procedure described in Eq. 2 is equivalent to a numerical filter with the filter function

$$H^2 = \sin^4 \left\{ \frac{\omega \cdot \Delta t}{2} \right\} / \left(\frac{\omega \cdot \Delta t}{2} \right)^2, \quad (3)$$

with ω as the angular frequency. The filter function, a hypothetical $-5/3$ energy distribution and the energy seen by the analysis described are shown in Figure 1. Assuming that the gravity wave energy is really distributed according to the $-5/3$ law (e.g. Manson et al., 1997), the Collm measurements see about 20% of the energy in the period range 0.5-6 h, which is equivalent to the ratio between the areas below the solid and dashed lines in Figure 1.

From the analysis of variances at one point the propagation direction of single waves cannot be inferred, but it is possible, to estimate the preferred propagation direction (e.g. Gavrilov et al., 1995). If we write:

$$\xi' = u' \sin \varphi + v' \cos \varphi, \quad (4)$$

with φ being the direction vs. North, we obtain for the total variance ξ'^2 in the direction φ .

$$\overline{\xi'^2} = \overline{u'^2} \sin^2 \varphi + \overline{v'^2} \cos^2 \varphi + r \sqrt{\overline{u'^2 v'^2}} \sin 2\varphi, \quad (5)$$

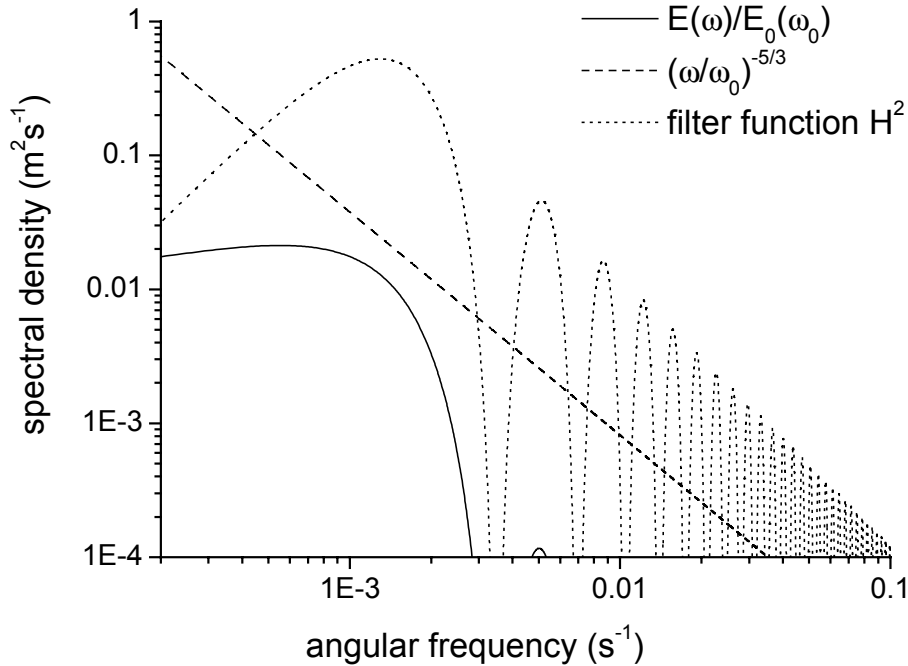


Figure 1: Filter function H^2 given in Eq. 3. A $-5/3$ energy distribution is added, scaled to an energy E_0 at $\omega_0 = 12.5$ h, and the contribution E/E_0 that is seen by the measurements and data analysis.

with r as the correlation coefficient between u' and v' . Eq. 5 describes an ellipse, with the direction of the main axis as the preferred propagation direction to be calculated by differentiating Eq. 5 with respect to φ .

$$\varphi_{pref} = \frac{1}{2} \left(n\pi + a \tan \frac{2r\sqrt{u'^2 v'^2}}{v'^2 - u'^2} \right), \quad (6)$$

with $n = 1$ if the denominator in Eq. 6 is negative, and $n = 0$ for $r > 0$ or $n = 2$ for $r < 0$, respectively, if the denominator in Eq. 6 is positive. One should keep in mind that Eq. 6 gives the angle of inclination of the main axis of the wind variance oval, which corresponds to the line of propagation of main wave component. These components may propagate in both directions along this line, therefore, this analysis can not give information about their actual directions.

Height measurements are available since September 1982, but during the first year of measurements the data density was low so that only hourly means have been constructed that do not allow to check the precondition of $\Delta h \leq 2$ km. Therefore we use data between 12/1983 and 11/2003 for the analysis. The number of data points with $\Delta h \leq 2$ km during 12/1983 and 11/2003 binned in months, and each value representing a 10 km height interval, is shown in Figure 2. Since during daylight hours especially in summer months data gaps appear due to the strong D-region absorption, the total number of GW data is larger in winter.

For comparison, the mean background drift velocities u_0 and v_0 are calculated as the average u and v during the respective time intervals. Note that these mean winds are not equivalent to the prevailing winds shown e.g. by Schminder and Kürschner (1994) or Schminder et al. (1997), since here we do not perform a decomposition into mean and tidal winds and the data are unevenly distributed during the day so that the average of the measured winds not necessarily equals the real mean.

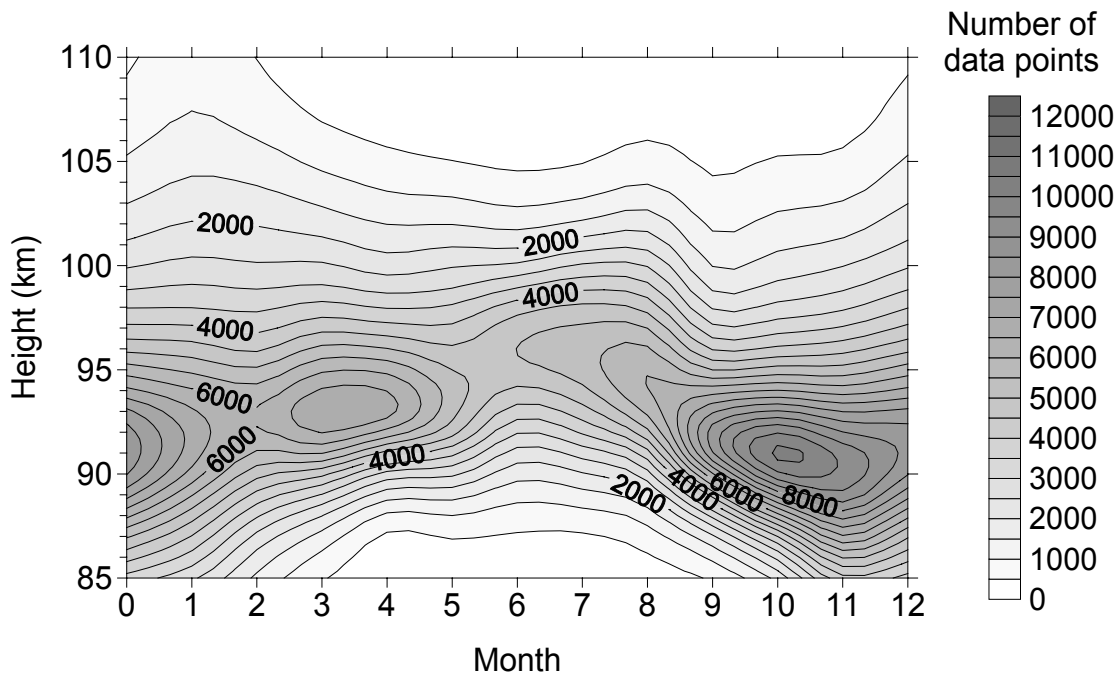


Figure 2: Number of data points per 10 km height range during the 20-year time interval 12/1983-11/2003 in the respective month .

20-year mean results

The 20-year averages of the variance u'^2 of the zonal drift component for each month of the year are shown in the left panel of Figure 3. The respective background drift velocities u_0 , i.e. the 20-year averages of u for each month are added as contour lines. The results for u'^2 confirm earlier results presented by Gavrilov et al. (2001) using the same dataset, but for a shorter time interval. The mean variances show a summer maximum in the upper mesosphere, which is replaced by a SAO with minima near the solstices in the lower thermosphere. Note that in the uppermost and the lowermost layers the measuring density is small (cf. Figure 2), however, the standard deviation of the individual monthly means (not shown here) is still smaller than the seasonal cycle at these heights, so that the results are least qualitatively reliable. The mesospheric summer maximum may be explained by the strong mean zonal winds there, which lead to large intrinsic phase velocities and hence, assuming a saturated gravity wave spectrum, to larger amplitudes (Manson et al., 1997). While the long-term mean winter mesospheric jets are weaker (see e.g. Schminder et al., 1997), the winter GW amplitudes are smaller than the summer ones. However, literature results even for similar latitudes show that there generally is a SAO in the upper mesosphere (Manson and Meek, 1993; Manson et al., 1999, 2003, 2004), which is more or less absent in the variances over Collm. The weaker winter GW activity over Collm may be consistent with weaker mean winter zonal winds there than over Canada (Jacobi et al., 2001).

Comparison of u'^2 and u_0 in Figure 3 show the correlation of the u'^2 maximum with the time of maximum vertical background wind gradient seen in summer near altitude 85 km. The Figure, however, is constructed from monthly profiles of u'^2 and u_0 so that the similarity of the structures is mainly owing to the May profile. During the other summer months both u'^2 and the vertical background wind gradients decrease monotonically with height so that no final conclusion can be drawn on a possible correlation.

Figure 3 shows also the mainly annual cycle of u_0 at altitudes 85–90 km and its semiannual variation above 100 km with maxima of eastward flow in winter and summer. This is connected with penetration of westward circulation of the middle atmosphere up to altitudes of 110 km in March–April. Semiannual variations of u_0 and related wind gradients above 100 km may cause semiannual variations of u'^2 seen in the upper part of Figure 3. Similar altitude variations of u_0 and u'^2 were observed by Gavrilov et al. (2004) over Hawaii, but there the semiannual variations are found at lower altitudes.

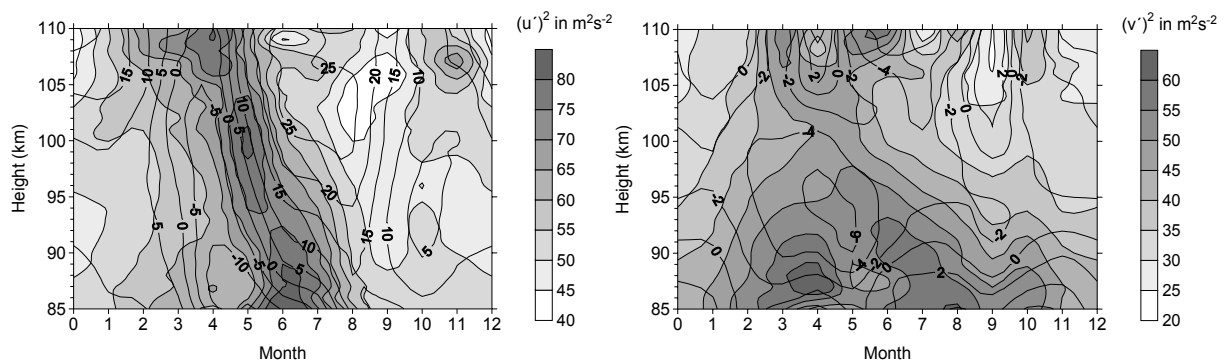


Figure 3: Height-time cross-section of 20-year mean variances for each month of the year (grey scaling). Contours show the 20-year mean background winds. Left panel: zonal component. Right panel: meridional component.

A limitation of LF measurements has to be mentioned here. During the half-hour intervals used for the analysis we average over about 60 individual measurements of wind, and attribute the resulting mean to the mean height analysed then. Therefore, in the presence of strong vertical wind shear and simultaneously stronger short-periodic variations of the reflection height the variance of half hourly drift means increases, which could be responsible for somewhat increased variance between two consecutive measurements also. This may lead to overestimated summer values of variances. However, the seasonal peculiarities, in particular the nonexistent second maximum in winter, cannot be explained by that, since vertical background wind gradients are smallest during equinoxes. Therefore we may conclude that the results should be correct at least qualitatively.

The mean meridional drift v_0 and its variance v'^2 are shown in the right panel of Figure 3. No clear correlation of v'^2 with the background meridional wind profile is visible here. This is due to the fact that strong zonal winds also increase the intrinsic phase speeds of waves with a meridional component, so that a more close correlation is expected with the zonal background winds. As expected, the general seasonal and altitudinal distribution of v'^2 in Figure 3 is similar to the climatology of the zonal variance component show in the left panel.

From the statistics of wind variability perturbation ellipses have been calculated using Eq. 5 and they are presented in are shown in Figure 4. The inclination angles ϕ_{pref} of lines of preferred propagation of major waves obtained after Eq. 6 are also added. Nominal centres of the height intervals considered are 85, 90, 95, 100, and 105 km. Due to the uneven distribution of the data the real mean heights, presented on the right of each curve, are different from these nominal heights.

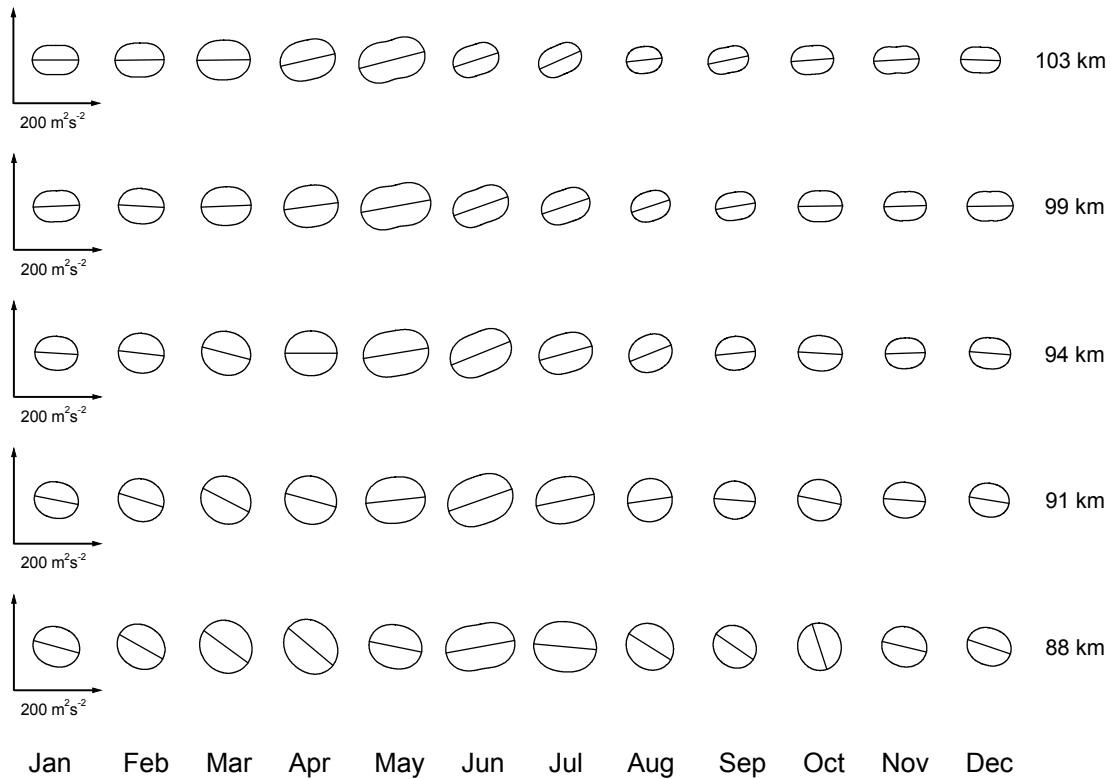


Figure 4: *Perturbation ellipses for each month of the year for different 10 km height intervals centred at 85, 90, 95, 100, and 105 km. The numbers given on the right of the respective row show the real mean heights of the data used. The length of the arrows shown on the left-hand side of the panels indicate a variance of $200 \text{ m}^2 \text{ s}^{-2}$.*

The propagation direction as is shown in Figure 4 is generally E-W, however, during winter at lower heights a more South-Easterly direction is preferred, while at greater heights during summer a North-Easterly direction is visible. At the upper heights regarded here the aspect ratio of the ovals increases, indicating a stronger orientation of GW towards their preferred propagation direction. The annual direction variation is comparable to some of the values presented in literature. Manson et al. (2003) showed mean ellipses for Saskatoon (52°N , 107°E) for the time interval July 2000 through December 2001. Their longer period (2-6 hrs) GW show a similar behaviour as we find for our lower heights. However, the filters they used are somewhat different from the one shown in Figure 1, and only qualitative agreement may be stated. Perturbation ellipses over Saskatoon shown for other years (Manson et al., 1997), however, reveal a more pronounced N-S orientation. The same is the case with data from Scandinavian radars taken during summer months (Hall et al., 2003; Manson et al., 2004). However, long-term analyses of Saskatoon data performed by Gavrilov et al. (1995) had shown preferred E-W orientation for the upper layers covered by MF radar. It may be concluded that comparison of long-term analyses with single or few-years results is not suitable, and GW directions may show strong interannual variations.

Interannual and decadal variability

Time series of seasonal (3-monthly) mean zonal drift variances are shown in Figure 5. Here, each “monthly” value refers to a 3-monthly mean, i.e. “December 1983” means 11/83-01/84, etc. The respective meridional variance values are shown in Figure 6. To avoid a possible influence of geomagnetic disturbances on the results, only data measured during days with the daily index of magnetic disturbance, $A_p < 20$ has been considered here. Maximum values are visible around 1989-1991 and 2000-2002, which is concomitant with the solar activity maxima within the 11-year solar cycle. This correspondence is visible in each season and for both horizontal variance components. This confirms results obtained with the MU radar over Shigaraki, Japan (Gavrilov et al., 1999), however, Gavrilov et al. (1995) have found negative correlation between the solar flux and GW activity over Saskatoon, Canada, for the same latitude. This difference of interannual variability over two stations very similar in latitude but different in longitude has already been stressed by Gavrilov et al. (2002).

A possible explanation of GW decadal variability may be the different mean winds and wind shear in the mesosphere. Bremer et al. (1997) and Jacobi (1998) have shown that during solar maximum the lower thermosphere easterly mean winds are weaker, while the vertical positive wind gradient is stronger, which is equivalent to a stronger mesospheric easterly jet (Schminder et al., 1997). This is confirmed by modelling results (Balachandran and Rind, 1995; Kodera et al., 2003; Fröhlich et al., 2004) who showed that during solar maximum both the summer and winter middle atmosphere jets are stronger than during solar minimum. Little is known, however, whether the spring and autumn middle atmosphere circulation also shows similar solar effect. MLT wind measurements indicate that the April and May zonal winds are negatively correlated with the sunspot number (Bremer et al., 1997; Jacobi, 1998). Strictly speaking, however, the month of May cannot be considered as a spring month, and the three-monthly MAM data in Figure 5 and Figure 6 represent a mixture of late winter, spring and early summer, the latter again with a considerable zonal wind jet in the mesosphere. No clear solar cycle effect has been reported for Collm autumn zonal mean winds (Bremer et al., 1997; Jacobi, 1998), however, again the 3-monthly means presented here include data with summer, autumn, and winter characteristics.

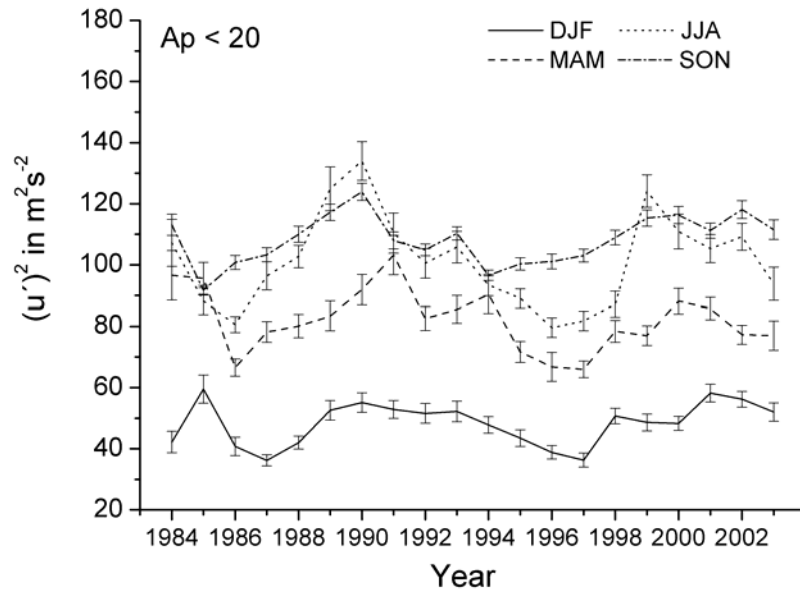


Figure 5: Time series of seasonal mean zonal wind variance u'^2 for 4 seasons. Nominal height is 90 km, mean height is 91.3 km. DJF values refer to the year of the respective December. Only data from days with $A_p < 20$ has been used. DJF values are correct, MAM, JJA and SON data are shifted by $20 \text{ m}^2 \text{ s}^{-2}$ each.

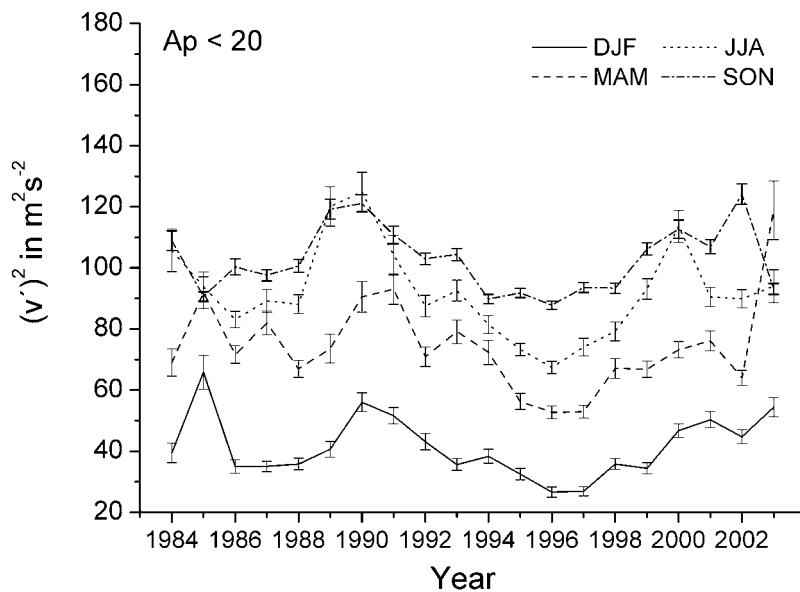


Figure 6: As in Figure 5, but for the meridional wind variance component.

In any case, if we consider the decadal GW activity changes as a signal of the 11-year solar cycle, we find that this signal is obviously stronger than the relatively weak solar signal in the MLT winds. This may be explained by applying simple linear theory (e.g. Andrews et al., 1987) for a saturated wave. In this case the geopotential amplitude is proportional to the inverse vertical wavenumber squared and hence to the intrinsic phase speed squared. Therefore the small solar signal in the background circulation is magnified when GW time series are considered. Correlation coefficients of the total variance $u'^2 + v'^2$ vs. sunspot number are given in Table 1 (2nd column). The correlation is significant at the 95% level except for MAM.

Table 1: Correlation coefficients between $u'^2+v'^2$ and the 3-monthly mean sunspot number for 4 seasons for undisturbed ($A_p < 20$), disturbed ($A_p \geq 20$) and all days. Database is 12/1983-11/2003. The long-term mean, calculated from the 20 seasonal means is also added. * In 1996 and 1997 less than 10 values were obtained in JJA, so these years were not included in the analysis. ** modified values without including 1996 and 1997.

Season	undisturbed		all data		disturbed	
	r	Mean	r	Mean	r	Mean
DJF	0.55	89.7	0.63	91.3	0.51	99.0
MAM	0.44	116.6	0.51	118.8	0.64	125.2
JJA	0.82	113.5 (118.2**)	0.83	115.3 (120.1**)	0.51	131.6*
SON	0.76	91.1	0.73	92.5	0.63	98.2

When analysing solar variability on MLT wind variances, one has to take into account possible effects of the solar cycle especially during strong magnetospheric storms on reflection heights within the half-hourly sampling intervals, which, in the presence of vertical wind gradients may give rise to apparent wind variances. This cannot be excluded even when only quiet or moderate geomagnetic conditions are considered. However, increased height variance will affect the half-hourly mean wind variance above all in the presence of large vertical gradients and large absolute wind values. Since the vertical gradient of the zonal mean winds are much stronger than the gradients of the meridional wind, this would mean that the apparent solar cycle would be more expressed in the zonal component than in the meridional one. However, from Figure 5 and Figure 6 one can infer that this is not the case, so we may conclude that the decadal variation of drift variance is not due to background wind vertical gradients.

In addition, earlier analyses of vertical soundings (Weiss, 1973) had shown that a tendency of the ionospheric layers to disintegrate (which enhances strong scatter of reflection height) has a seasonal cycle with minima in spring and autumn, which is not reflected in the correlations given in Table 1. To obtain an idea about the possible influence of geomagnetic disturbances on measured drift variances, in Table 1 correlation coefficients are also given for disturbed conditions ($A_p \geq 20$) and the entire dataset. The solar cycle variability is preserved and no obvious dependence on geomagnetic disturbance is visible, so we may conclude that the solar cycle effects visible in the data may, at least qualitatively, be owing to GW activity. However, Table 1 also shows that during geomagnetically disturbed days the mean variance is somewhat larger on average. We cannot distinguish whether this is an effect of increased GW, or an effect within the half-hourly time scale. Hall et al. (2002) showed a weak increase of turbulence during geomagnetically disturbed conditions, which may influence our results.

Considering interannual variations at shorter time scales, Gavrilov et al. (1999) have presented GW analyses from MU radar data. In their analysis some indication of an influence of El Nino on the interannual variability of GW activity are visible. A more pronounced correlation of GW activity with the Southern Oscillation Index (SOI) was presented by Gavrilov et al. (2004) using MF radar data over Hawaii. Visual inspection of the interannual variability of GW over Collm in Figure 5 and Figure 6 reveals some local maxima in the years 1992–1994 and 1998, which could correlate with strong El-Nino events. However, the decadal variability

of drift variances is obviously stronger than other interannual variations, and there is no significant correlation of SOI with Collm GW activity near 91 km. This may indicate that a possible SO influence on the MLT GW activity is stronger at low latitudes, which is consistent with a stronger GW control by their lower atmosphere sources at low latitudes (Manson et al., 1999). Possible weaker signals of SO influence on GW activity in the upper atmosphere of middle latitudes requires further analysis.

Conclusions

We have used a dataset of 20 years of MLT lower E-region drift data to analyse the climatology of atmospheric gravity waves and their seasonal and interannual variability. The seasonal variability to a certain degree confirms results from earlier work and is also in correspondence with literature results for other stations. However, much information on GW in the MLT region is available from medium frequency radars, whose measurements are usually limited in height to a maximum of about 95 km, so that we do not have much information to compare with the upper layers considered here. In turn, the upper mesosphere between 60-80 km that can be covered by other radars is not seen here. Since the seasonal variation of GW is strongly height-dependent, comparisons of the results with data presented in literature have to be made with care.

Clearly, GW activity in the MLT is not only modified through middle atmosphere wind filtering, but also by GW sources. Comparison of the mean climatology with those derived from measurements at other sites must therefore show differences that in many cases cannot be explained as the GW source functions are not known. Global measurements at lower stratospheric heights (e.g. Tsuda et al., 2000; Venkat Ratnam et al., 2004) are therefore necessary if GW climatologies are used e.g. for validation of model results.

Due to the specific limitations of the LF method, analysis of interannual variability is only possible for a limited height range near the maximum measuring density height. The major variation in the interannual and decadal time scale is a clear decadal oscillation in phase with the 11-year solar cycle, which may be explained by the effect of the mesospheric jets on GW propagation and saturation. This 11-year variation signal is stronger than the one that has been visible in MLT prevailing winds (e.g. Jacobi 1998), so that GW variability may be taken as an indicator for middle atmosphere long-term variations.

A significant influence of ENSO is not visible in the data at 85-95 km. Although a possible SO influence on the MLT GW activity may as well be dependent on height, the to a certain degree preliminary results indicate that an ENSO effect on MLT GW may be mainly constrained to lower and lower middle latitudes. To draw more substantial conclusions for middle latitudes, however, requires further investigation of the data in comparison with other measurements and model results.

Acknowledgements: This study has been partly supported by INTAS under grant INTAS 03-51-5380.

References

Balachandran, N.K., and D. Rind, 1995: Modeling the effects of UV variability and the QBO on the troposphere-stratosphere system. Part I: The middle atmosphere. *J. Clim.* 8, 2058-2079.

- Bremer, J., R. Schminder, K.M. Greisiger, P. Hoffmann, D. Kürschner, and W. Singer, 1997: Solar cycle dependence and long-term trends in the wind field of the mesosphere/lower thermosphere. *J. Atmos. Solar-Terr. Phys.* 59, 497-509.
- Fröhlich, K., und Ch. Jacobi, 2004: The solar cycle in the middle atmosphere: changes of the mean circulation and of propagation conditions for planetary waves. *Rep. Inst. Meteorol. Univ. Leipzig* 34, 106-117.
- Gavrilov, N.M., A.H. Manson, and C.E. Meek, 1995: Climatological monthly characteristics of middle atmosphere gravity waves (10 min - 10 h) during 1979-1993 at Saskatoon. *Ann. Geophysicae* 13, 285-295.
- Gavrilov, N.M., S. Fukao, and T. Nakamura, 1999: Peculiarities of interannual changes in the mean wind and gravity wave characteristics in the mesosphere over Shigaraki, Japan. *Geophys. Res. Lett.* 26, 2457-2460.
- Gavrilov, N.M., and S. Fukao, 2001: Hydrodynamic tropospheric wave sources and their role in gravity wave climatology of the upper atmosphere from the MU radar observations. *J. Atmos. Solar-Terr. Phys.* 63, 931-943.
- Gavrilov, N.M., Ch. Jacobi and D. Kürschner, 2001: Short-period variations of ionospheric drifts at Collm and their connection with the dynamics of the lower and middle atmosphere. *Phys. Chem. Earth* 26, 459-464.
- Gavrilov, N.M., S. Fukao, T. Nakamura, Ch. Jacobi, D. Kürschner, A.H. Manson and C.E. Meek, 2002: Comparative study of interannual changes of the mean winds and gravity wave activity in the middle atmosphere over Japan, Central Europe and Canada. *J. Atmos. Solar-Terr. Phys.* 64, 1003-1010.
- Gavrilov, N.M., and Ch. Jacobi, 2004: A study of seasonal variations of gravity wave intensity in the lower thermosphere using LF D1 wind observations and a numerical model. *Ann. Geophysicae* 22, 35-45.
- Gavrilov, N.M., D.M. Riggin, and D.C. Fritts, 2004: Interannual variations of the mean wind and gravity wave variances in the middle atmosphere over Hawaii. *J. Atmos. Solar-Terr. Phys.* 66, 637-645.
- Hall, C.M., S. Nozawa, C.E. Meek, and A.H. Manson, 2002: On the response of fading times of upper homosphere radar echoes to solar and geomagnetic disturbances. *Earth Planets Space* 54, 699-705.
- Hall, C.M., T. Aso, A.H. Manson, C.E. Meek, S. Nozawa, and M. Tsutsumi, 2003: High-latitude mesospheric mean winds: A comparison between Tromsø (69°N) and Svalbard (78°N). *J. Geophys. Res.* 108, 4598, doi: 10.1029/2003JD003509.
- Jacobi, Ch., 1998: On the solar cycle dependence of winds and planetary waves as seen from midlatitude D1 LF mesopause region wind measurements. *Ann. Geophysicae* 16, 1534-1543.
- Jacobi, Ch., M. Lange, D. Kürschner, A.H. Manson and C.E. Meek, 2001: A long-term comparison of Saskatoon MF radar and Collm LF D1 mesosphere-lower thermosphere wind measurements. *Phys. Chem. Earth* 26, 419-424.
- Kodera, K., K. Matthes, K. Shibata, U. Langematz, and Y. Kodera, 2003: Solar impact on the lower mesospheric subtropical jet: A comparative study with general circulation model simulations. *Geophys. Res. Lett.* 30, 1315, doi: 10.1029/2002GL016124.
- Kürschner, D., 1975: Konzeption und Realisierung eines vollautomatischen Registriersystems zur Durchführung von nach der D1-Methode angelegten Routinebeobachtungen ionosphärischer Driftparameter am Observatorium Collm. *Z. Meteorol.* 25, 218-221.
- Kürschner, D., R. Schminder, W. Singer and J. Bremer, 1987: Ein neues Verfahren zur Realisierung absoluter Reflexionshöhenmessungen an Raumwellen amplitudenmodulierter Rundfunksender bei Schrägeinfall im Langwellenbereich als Hilfsmittel zur Ableitung von Windprofilen in der oberen Mesopausenregion. *Z. Meteorol.* 37, 322-332.

- Manson, A.H., and C.E. Meek, 1993: Characteristics of gravity waves (10min-6h) at Saskatoon (52°N, 107°W): Observations by the phase coherent medium frequency radar. *J. Geophys. Res.* 98, 20357-20367.
- Manson, A.H., C. E. Meek and Q. Zhan, 1997: Gravity wave spectra and direction statistics for the mesosphere as observed by MF radars in the Canadian prairies (49°N-52°N) and at Tromsø (69°N). *J. Atmos. Solar-Terr. Phys.* 59, 993-1009.
- Manson, A.H. C.E. Meek, C. Hall, W.K. Hocking, J. MacDougall, S. Franke, K. Igarashi, D. Riggan, D.C. Fritts, and R.A. Vincent, 1999: Gravity wave spectra, directions and wave interactions: Global MLT-MFR network. *Earth Planets Space* 51, 543–562.
- Manson, A.H., C.E: Meek, S.K. Avery, and D. Thorsen, 2003: Ionospheric and dynamical characteristics of the mesosphere-lower thermosphere region over Platteville (40°N, 105°W) and comparisons with the region over Saskatoon (52°N; 107°W). *J. Geophys. Res.* 108, doi: 10.1029/2002JD002835.
- Manson, A.H., C.E. Meek, C.M. Hall, S. Nozava, N.J. Mitchell, D. Pancheva, W. Singer, and P. Hoffmann, 2004: Mesopause dynamics from the Scandinavian triangle of radars within the PSMOS-DATAR Project. *Ann. Geophysicae* 22, 367-386.
- McLandress, C., M.J. Alexander, and D.L. Wu, 2000: Microwave Limb Sounder observations of gravity waves in the stratosphere: A climatology and interpretation. *J. Geophys. Res.* 105, 11947-11967.
- Nastrom, G.D., and D.C. Fritts, 1992a: Sources of mesoscale variability of gravity waves. Part I: Topographic excitation. *J. Atmos. Sci* 49, 101-110.
- Nastrom, G.D., and D.C. Fritts, 1992b: Sources of mesoscale variability of gravity waves. Part II: Frontal, convective, and jet stream excitation. *J. Atmos. Sci.* 49, 111-127.
- Schminder, R., and D. Kürschner, 1994: Permanent monitoring of the upper mesosphere and lower thermosphere wind fields (prevailing and semidiurnal tidal components) obtained from LF D1 measurements in 1991 at the Collm Geophysical Observatory. *J. Atmos. Terr. Phys.* 56, 1263–1269.
- Schminder, R., Ch. Jacobi, D. Kürschner, P. Hoffmann, D. Keuer and W. Singer, 1997: The upper mesosphere and lower thermosphere wind field over Central Europe from 1994 through 1996 obtained from a joint analysis of LF windprofiler and MF radar measurements. *Meteorol. Zeitschrift*, N.F. 6, 225-229.
- Taylor, M.J., E.H. Ryan, T.F. Tuan, and R. Edwards, 1993: Evidence of preferential directions for gravity wave propagation due to wind filtering in the middle atmosphere. *J. Geophys. Res.* 98, 6047-6057.
- Tsuda, T., M. Nishida, C. Rocken, and R.H. Ware, 2000: A global morphology of gravity waves by GPS/MET data. *J. Geophys. Res.* 105, 7252 - 7273.
- Venkat Ratnam, M., G. Tetzlaff and Ch. Jacobi, 2004: Global and seasonal variations of stratospheric gravity wave activity deduced from the CHALLENGING Minisatellite Payload (CHAMP)-GPS Satellite. *J. Atmos. Sci.* 61, 1610-1620.
- Weiß, E., 1973 : Methode und Ergebnisse der ionosphärischen Impulsotung mittels elektromagnetischer Wellen auf 314.5 und 185 kHz, Diss. Univ. Rostock.

Addresses of Authors:

- Christoph Jacobi, Institut für Meteorologie, Universität Leipzig, Stephanstr. 3, 04103 Leipzig, jacobi@uni-leipzig.de
- Dierk Kürschner, Institut für Geophysik und Geologie, Observatorium Collm, 04779 Wernsdorf, kuersch@uni-leipzig.de
- Nikolai M. Gavrilov, Atmospheric Physics Department, Physical Research Institute, Saint-Petersburg State University, 1 Ul'yanovskaya Street, Petrodvorets, Saint Petersburg, 198904, Russland, gavrilov@pobox.spbu.ru